

## Numerical Simulation of Flow through Sukhoi 24 Air Inlet

Mostafa Mahmoodi<sup>a</sup>, Kiumars Khani Aminjan<sup>b\*</sup>

<sup>a</sup> Malek Ashtar University of Technology, Aerospace University Complex, Tehran, Iran

<sup>b</sup> Young Researchers and Elite Club, Islamic Azad University, Astara Branch, Astara, Iran

Keywords	Abstract
Sukhoi 24, Air inlet, Pressure reduction, Pressure efficiency, Distortion.	All motors in jets have an inlet part for bringing free air into motor which we call it inlet duct. Inlet duct is placed before compressor and has considerable impact on thrust amount. It is in various shapes and sizes which each one has specific characteristics with respect to motor and airplane speed. But, their common characteristics include having the lowest pressure reduction and the lowest distortion. In this paper, the air inlet of a fourth generation warplane (Sukhoi 24) is considered for the numerical simulation. Then, with regard to its motor characteristics according to Jane's aero-engines and with respect to experimental relations and existed plans, its air inlet is modeled and numerically analyzed by FLUENT software. With regard to the conducted analysis for $H=0$ and obtaining 1.07 for Mach number, air inlet will be analyzed in two conditions: subsonic and supersonic. More pressure reduction and more distortion have been observed in the subsonic condition. Of course, with respect to the nature of Sukhoi 24 which is a raptor warplane, it is expected that desirable results can be obtained for supersonic condition (The efficiency was 98.64% and distortion was about 0.32).

### 1. Introduction

All jet engines have an inlet to bring free stream air into the engine. The inlet sits upstream of the compressor and, while the inlet does no work on the flow, there are some important design features of the inlet. The air intake is that part of an aircraft structure by means of which the aircraft engine is supplied with air taken from the outside atmosphere. The air flow enters the intake and is required to reach the engine face with optimum levels of total pressure and flow uniformity. These properties are vital to the performance and stability of engine operation [1]. Depending on the type of installation, this stream of air may pass over the aircraft body before entering the intake properly. Selection of the correct type of intake and the associated intake geometry has important consequences to any airplane design. For this reason, intake design receives considerable attention in the design phase of an airplane. Intakes come in a variety of shapes and sizes with the specifics usually dictated by the speed of the aircraft. An engine's air intake duct is normally considered an airframe part and made by aircraft manufacturer. During the flight operation, it is very important for the engine performance. Engine thrust can be high only if the intake duct supplies the engine with the required airflow at the highest possible pressure. Intakes must be able to recover as

much of the total pressure of the free air stream as possible and deliver this pressure to the front of the engine compressor. The duct must deliver air to the compressor under all flight conditions with a little turbulence. As far as the aircraft is concerned, the duct must hold to a minimum of the drag [1]. The duct also usually has a diffusion section just ahead of the compressor to change the ram air velocity into higher static pressure at the face of the engine. This is called ram recovery. The intake duct is built generally in the divergent shape (subsonic diffuser). The problem of air intake design is to ensure that an aircraft engine is properly supplied with air under all conditions of aircraft operation and that the aptitude of the airframe is not unduly impaired in the process [2]. The geometry used in this study is Sukhoi 24 air inlet, and the geometry of the air intake first was designed and then was analyzed by FLUENT software.

### 2. Literature Background

Papamoschou [3] presented a simple theoretical method to determine the inviscid steady state diffuser performance of a tunnel with two plane, parallel supersonic streams that come into constant downstream of a splitter plane and from an infinitely thin interface. Singh et al. [4] presented a study of the field of axisymmetric, mixed compression, supersonic

\* Corresponding Author:

E-mail address: [kiomars.khani67@gmail.com](mailto:kiomars.khani67@gmail.com) – Tel, (+98) 9117222988

Received: 21 October 2016; Accepted: 28 January 2017

air intakes for viscous flows. The governing equations of mass, momentum, energy and state equation have been solved to obtain the complete flow field using the commercial software package (FLUENT). Recently, CFD was used for supersonic inlet [2, 5-7]. Mohler [8] proposed the flow simulations over the M2129 diffusing S-duct with and without vane effectors were computed by the Wind-US flow solver. The Wind-US code is used to predict total pressure recovery and distortion in a diffusing serpentine engine inlet duct, which are the two parameters that characterize the aerodynamic effectiveness of an engine inlet. CFD software was used for the simulations and the results are compared with the experimental results. The experimental program investigated the control of total pressure recovery and distortion at the engine face of a serpentine inlet. Flow control was attempted by installing rings of vane effectors, sometimes referred to as vortex generators, around the sides of the duct. Calculations of total pressure recovery and distortion at the engine face, with and without flow control, agreed well with experiment. Smith et al. [9] obtained full Navier-Stokes calculations on the F/A-18A High Alpha Research Vehicle inlet for several angles of attack and free stream Mach numbers. The static pressure was studied along the surface of the inlet. The NPARC code, version 2.0 solves the full three dimensional Reynolds averaged Navier-Stokes equations. Necessary boundary conditions were given and the grids are generated. Although the NPARC results represent an asymptotic solution, it was able to capture the essential steady-state physics associated with the inlet flow field, which is inherently unsteady. The results were found for both internal and external flow. As the angle of attack increased, more of the external flow impacted on the inflow to the inlet.

Abrahamsent et al. [10], studied the flow in an S-shaped air intake using experimental and computational methods. In the experimental studies, they carried out the measurements of an isentropic light piston tunnel. And, in computational studies the non-linear eddy viscosity model was compared with a linear counterpart.

### 3. Inlet Analysis

In this study, flow through air inlet of Sukhoi 24 was analyzed. Sukhoi 24 (In Russian language: cy 24- Su 24-NATO: Fencer) is a strike fighter with two cabins, variable wings and tow motors manufactured by Sukhoi company which its propellants are two turbojet motor (SATURN/LYULKA AL-21F-3A) and their power are 109.8 Kilo-Newton.

The air inlet duct design process and analysis is conducted in an algorithm that its principles are to achieve the following objectives [11]

- 1- Supply the mass flow rate for propulsion system requirements.
- 2- Supplies required flow rate with minimal adverse distribution, static pressure and dynamic pressure.
- 3- The minimum total pressure loss.
- 4- Minimum flow rotational at the mouth of the inlet duct.

To draw geometry of air inlet in subsonic condition by using flying Mach number, cross the mouth of the inlet duct

(Fi) and various points of lip were calculated. In supersonic analysis, profile of geometry and ramp at the beginning of the air inlet mapped experimentally by using Sukhoi 24 images.



Figure 1. Sukhoi24

#### 3.1. Motor Type Selection

The type of the motor was selected according to Jane's aero engines [12], and with the following characteristics

Motor Diameter: 1020 mm

The maximum air flow entering to the motor:  $G = 104 \text{ kg/s}$ .

#### 3.2. Inlet Analysis for Subsonic Condition

For the subsonic condition, end point is a circle with a diameter similar to motor and air inlet has leap which experimental relations (Eq. (1)) will be applied for air inlet duct and leaps [11, 13].

$$H = 0, M = 0.95, \frac{G}{G_{th}} = 0.892 \rightarrow G_{th} = 116.592 \text{ kg/s} \quad (1)$$

In the above equations  $G_{th}$  is mass flow rate at throat. For throat area calculating, we use the following empirical relationships (Eqs. (2-8)) as

$$F_{th}^{cr} = \frac{G_{th} \sqrt{T_0}}{0.396 P_0 \delta} = 0.2768 \text{ m}^2 \quad (2)$$

$$F_{th} = \frac{F_{th}^{cr}}{\cos(15)} = 0.2865 \text{ m}^2 \quad (3)$$

$$d_{th}^h = \frac{\sqrt{4F_{th}}}{\sqrt{\pi}} = 604.040 \text{ mm} \quad (4)$$

For lower leap, we have

$$k = 10\% \rightarrow F_i = kF_{th} = 0.31515 \text{ m}^2 \quad (5)$$

$$d_i^h = \frac{\sqrt{4F_i}}{\sqrt{\pi}} = 633.452 \text{ mm} \quad (6)$$

$$Y = \frac{d_i^h - d_{th}^h}{2} = 14.706 \text{ mm} \quad (7)$$

$$X = 3Y = 44.118 \text{ mm} \quad (8)$$

**Table 1.** Points of lower leap for subsonic geometry

Points	1	2	3	4	5	6	7	8	9	10
X (mm)	2.205	4.411	8.823	13.235	17.647	22.050	26.407	30.882	35.294	44.118
Y (mm)	5.294	7.205	9.558	11.176	12.203	13.088	13.676	14.117	14.412	14.706

Calculations for the upper leap are presented in Eqs. (9) to (12) as below

$$K = 8\% \rightarrow F_i^h = KF_{th}^h = 0.30942 \text{ m}^2 \quad (9)$$

$$d_i^h = \frac{\sqrt{4F_i}}{\sqrt{\pi}} = 627.666 \text{ mm} \quad (10)$$

$$Y = \frac{d_i^h - d_{th}^h}{2} = 11.813 \text{ mm} \quad (11)$$

$$X = 3Y = 35.440 \text{ mm} \quad (12)$$

**Table 2.** Points of upper leap for subsonic geometry

Point	1	2	3	4	5	6	7	8	9	10
X(mm)	1.772	3.544	7.088	10.623	14.176	17.720	21.264	24.808	28.352	35.440
Y(mm)	4.253	5.788	7.678	8.978	9.805	10.513	10.986	11.304	11.576	11.813

According to the motor and airplane length, air inlet length will be 8 meters. The inlet geometry along with lip is presented in the Figure 2.

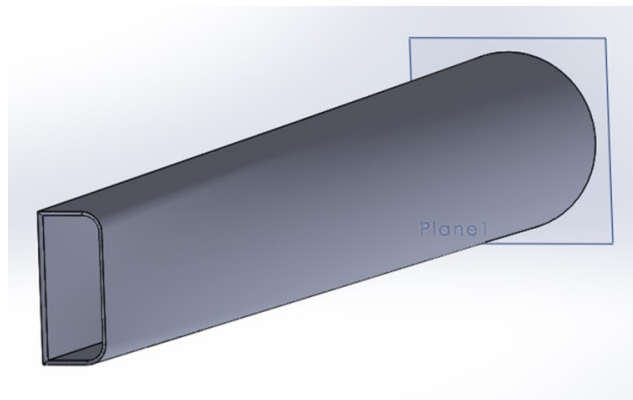


**Figure 2.** Geometry of air inlet for subsonic condition

For numerical analysis, the geometry must be meshed. In Figure 3, the meshed geometry of air inlet is shown in FLUENT software [14] environment.

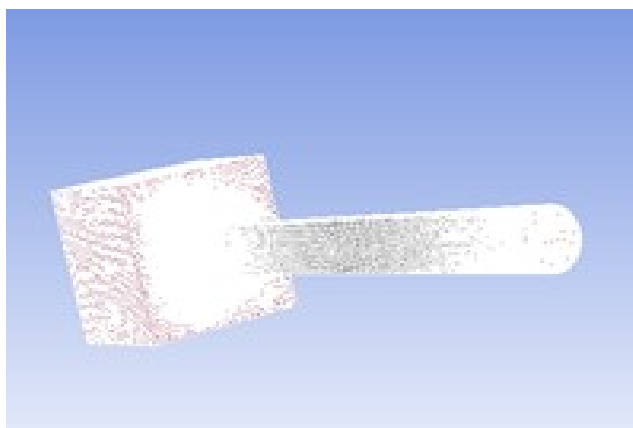


**Figure 3.** Meshed geometry for subsonic condition (cell numbers is 427376)

For analyzing with software, regarding to this fact that Mach is higher than 0.3, flow is compressive and density is not constant. Therefore, analysis was performed based on density. And, energy was also activated for presenting necessary equations. In addition, to analyze model, k-epsilon (realizable) was selected.

Figures 4 and 5 present the total pressure and Mach number in various points of inlet for subsonic condition. As indicated in these figures, the total pressure and Mach number through the inlet changes, however, because of several flow effects, the maximum Mach number and maximum total pressure are in the inlet and Mach number and total pressure are reduced during the air inlet duct. Aerodynamic characterizes the inlet's pressure performance by the inlet total pressure recovery, which measures the amount of the free stream flow conditions that are "recovered". the pressure recovery  $pt2 / pt0$  depends on a wide variety of factors, including the shape of the inlet, the speed of the aircraft, the airflow demands of the engine, and aircraft maneuvers. Recovery losses associated with the boundary layer on the inlet surface or flow separations in the duct are included in the inlet efficiency factor,  $n_i$ . The  $n_i$  is presented in Eq. (13) as

$$n_i = pt2/pt1 \quad (13)$$

For subsonic flight speeds, these losses are the only losses. For Mach number less than 1, the Military Specifications (Mil. Spec.) value of recovery is the inlet efficiency [15] as shown in the Eq. (14) below;

$$Mil. Spec., M < 1: pt2/pt0 = n_i \times 1 \quad (14)$$

For aircraft that cannot go faster than the speed of sound, like large airliners, a simple, straight, short inlet works quite well. On a typical subsonic inlet, the surface of the inlet from outside to inside is a continuous smooth curve with some thickness from inside to outside. The most upstream portion of the inlet is called the highlight, or the inlet lip. A subsonic aircraft has an inlet with a relatively thick lip. As indicated in Figure 6, the flow revolves around a lip and the lip prevented the flow separation at the edges therefore the lip increasing the total pressure recovery.

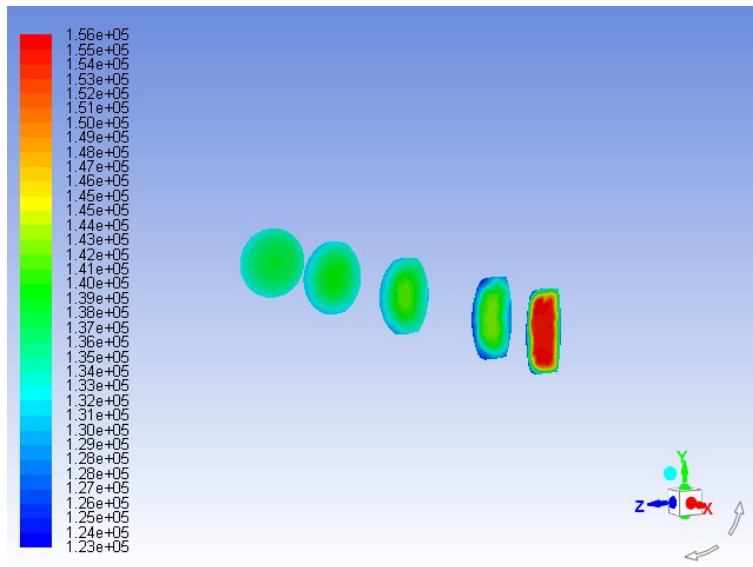


Figure 4. Total pressure in various points for subsonic condition

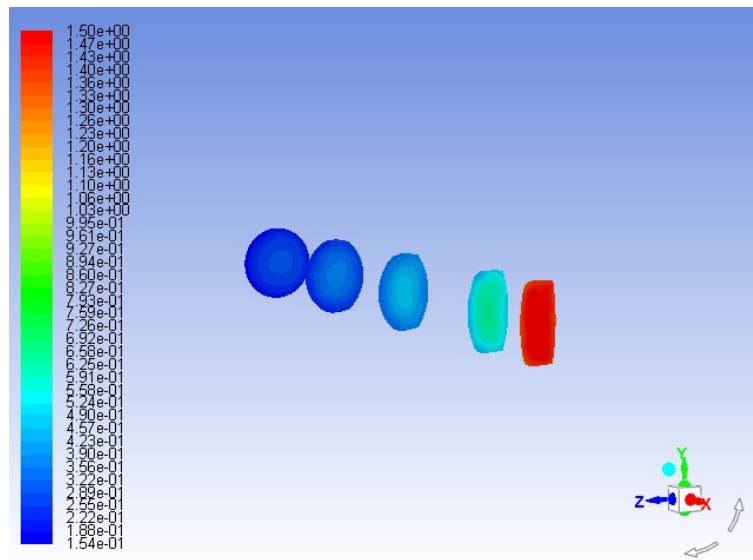


Figure 5. Mach number in various points for subsonic condition

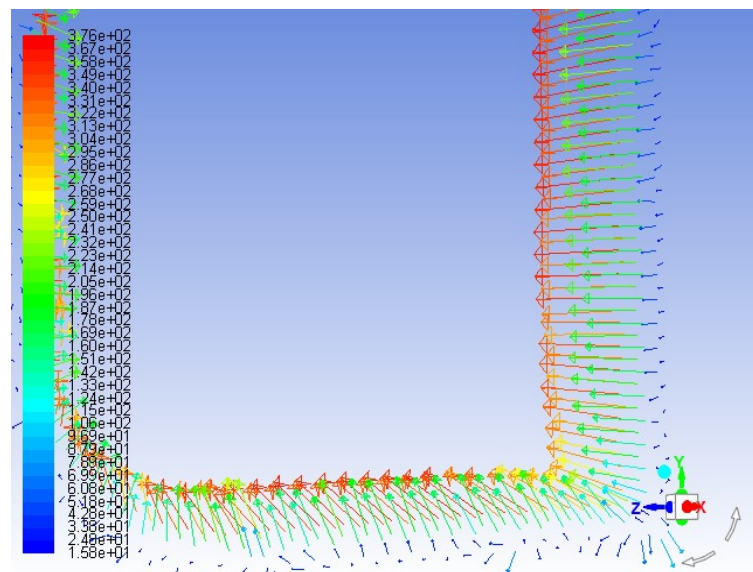


Figure 6. Speed vector in leap for subsonic condition

### 3.2.1. Analysis Results for Subsonic Condition

Performance analysis of each duct will be explained by two criteria including the total pressure output and distortion coefficient. In this study, because of compressive flow presence, Eq. (15) is used.

$$\eta_p = \frac{p_f}{p_\infty} = \frac{135702.8}{154425.8} \times 100 = 87.87\% \quad (15)$$

Eq. (16) is applied to calculate the total pressure distortion, and the pressure recovery coefficient was also obtained.

$$DC(\theta) = \frac{p_f - p_\theta}{q_f} = \frac{135702.8 - 132042.1}{5714.648} = 0.64 \quad (16)$$

where,  $P_f$  is the average of total pressure in motor inlet,  $q_f$  is the mean dynamic head, and  $P_\theta$  is the lower total pressure average in inlet points (with the angle  $\theta$ ). Summary of the results are presented in Table 3.

**Table 3.** Results for subsonic condition

Efficiency	Distortion	Input current Mach	Output current Mach	Input current total temperature (°k)	Output current total temperature (°k)	Input current static temperature (°k)	Output current static temperature (°k)	Input current density (kg/m <sup>3</sup> )	Output current density (kg/m <sup>3</sup> )
87.87%	0.64	0.79	0.24	324.74	324.12	288.16	320.07	1.22	1.41

### 3.3. Inlet Analysis for Supersonic Condition

In supersonic condition, inlet geometry is convergent-divergent, but since the Mach number is approximately 1, the geometry is convergent which is placed in front of ramp opening. In comparison to previous condition, this geometry is so similar to the geometry of air inlet in Sukhoi 24. Air inlet geometry along with ramp surface is shown in Figure 7.

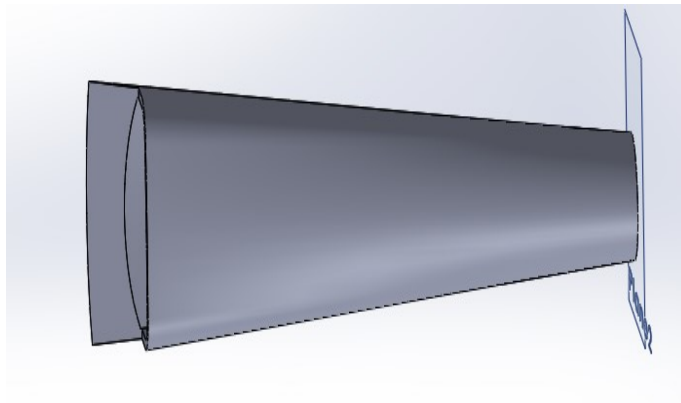


**Figure 7.** Geometry of inlet for supersonic condition

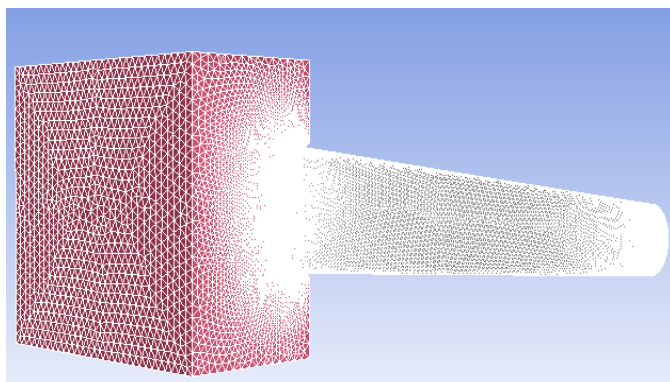


**Figure 8.** Meshed geometry for supersonic condition (cell numbers: 374083)

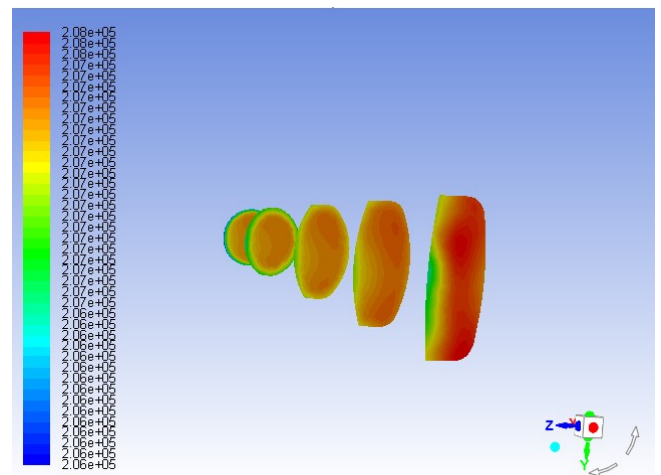


**Figure 9.** Total pressure in various points for supersonic condition

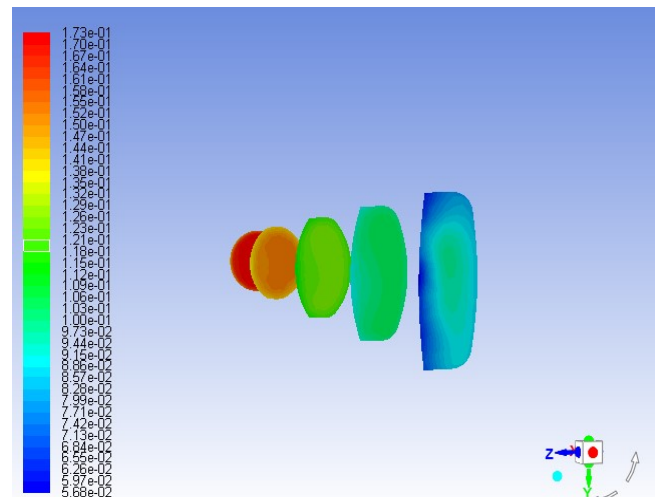


**Figure 10.** Mach number in various points for supersonic condition

Figures 9 and 10 present the total pressure and Mach number in various points of inlet for supersonic condition. Similar to the subsonic condition, the maximum Mach number and the maximum total pressure are in the inlet and the Mach and total pressure are reduced during air inlet duct. At supersonic flight speeds, there are additional losses

created by the shock waves necessary to reduce the flow speed to subsonic conditions for the compressor [15]. The inlet efficiency for this condition is presented as

$$Mil.Spec., M > 1: pt2/pt0 = n_i \times (1 - 0.075[M - 1]^{1.35}) \quad (17)$$

The Mil. Spec. loss is a good initial estimate of inlet recovery. Actual inlet performance may be greater, but is usually less than Mil. Spec. The magnitude of the recovery loss depends on the specific design of the inlet and is normally determined by wind tunnel testing.

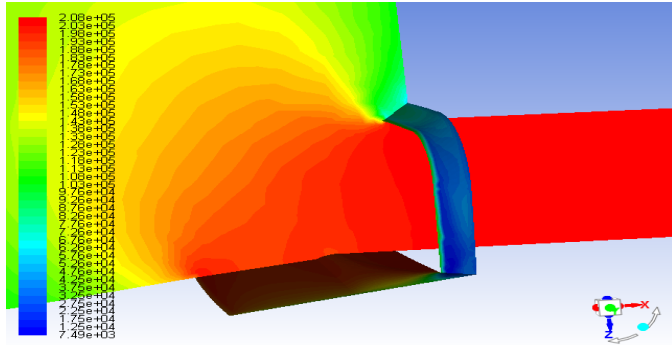


Figure 11. Static pressure contour on ramping surface for supersonic condition

Table 4. Results for supersonic condition

Efficiency	Distortion	Input current Mach	Output current Mach	input current of total temperature (°k)	Output current of total temperature	Input current static temperature (°k)	Output current static temperature (°k)	Input current density (kg/m <sup>3</sup> )	Output current density (kg/m <sup>3</sup> )
98.64%	0.32	1.044	0.16	353.48	353.97	290.15	351.95	1.25	2.009

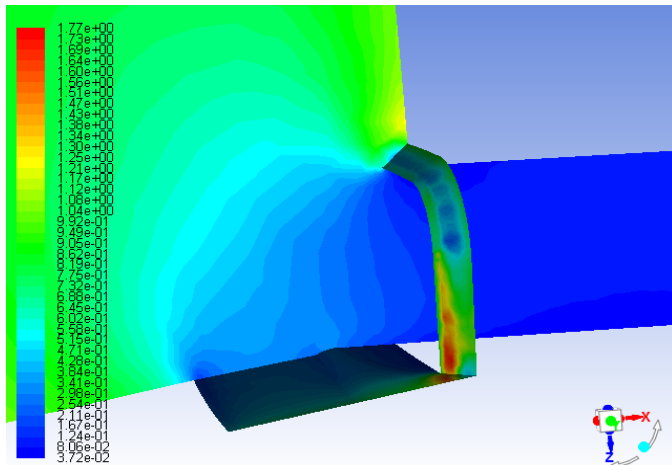


Figure 12. Mach Contour on Ramping Surface for supersonic condition

Comparing the results of the supersonic and subsonic conditions, showed a better results for supersonic condition.

#### 4. Conclusion

In this paper, the flow through air inlet of the Sukhoi 24 was numerically analyzed. Since analysis was performed for H = 0 and Mach was equal to 1.07, so the air inlet was analyzed in subsonic and supersonic conditions which this indicated more pressure drop and more distortion in subsonic condition. Of course, with respect to the nature of Shkhoi 24 which is a raptor, it was predicted that the results

According to the additional losses created by the shock waves in supersonic condition so to increase pressure recovery one of the methods is to use the ramp in front of inlet duct. Ramp with production oblique shocks reduces the pressure drop created by vertical shocks.in the top contours in Figures 11 and 12, immediate color changes in contours indicates the shock phenomenon. Shock caused a drastic change in the flow.

#### 3.3.1. Analysis Results for Supersonic Condition

Same to the subsonic condition, performance analysis of each duct will be explained by two criteria: the total pressure output and distortion coefficient (Eqs. (18) and (19))

$$\eta_p = \frac{p_f}{p_\infty} = \frac{205380.3168}{208212} \times 100 = 98.64\% \quad (18)$$

$$DC(\theta) = \frac{p_f - p_\theta}{q_f} = \frac{205380.3168 - 204081.8278}{4057.778} = 0.32 \quad (19)$$

The most pressure drop for an air inlet channel is lower than 0.02, so a desirable air inlet channel must have 98% pressure recovery or more [16].

for supersonic condition might be better (98.64% efficiency and 0.32 for distortion). It was observed that in subsonic condition, leap in the air inlet entrance prevented from flow separation in entry edge and reduced pressure drops. Also, in supersonic condition, the ramp in front of the entrance creates oblique shock and reduced the pressure drops in the entrance of inlet.

#### References

- [1] M.S. Prasath, CFD Study of air intake duct, 2014.
- [2] B.H. Anderson, J. Gibb, Application of CFD to the study of flow control for the management of inlet distortion, In 28th Joint Propulsion Conference and Exhibit (1992) 3177.
- [3] D. Papamoschou, Diffuser performance of two-stream supersonic wind tunnels, AIAA Journal 27 (1989) 1124–1127.
- [4] D.G. Roychowdhury, S.K. Das, T. Sundararajan, Numerical simulation of natural convective heat transfer and fluid flow around a heated cylinder inside an enclosure. Heat and mass transfer 38 (2002) 565–576.
- [5] J. Slater, CFD methods for computing the performance of supersonic inlets. In 40th AIAA/ASME/SAE/ASEE Joint Propulsion Conference and Exhibit (2004) 3404.
- [6] J.W. Slater, D.O. Davis, B.W. Sanders, L.J. Wier, Role of CFD in the Aerodynamic Design and Analysis of the Parametric Inlet. ISABE Paper, (2005) 1168.
- [7] J. Shigematsu, K. Yamamoto, K. Shiraishi, A. Tanaka, A numerical investigation of supersonic inlet using implicit TVD scheme. In: Proceedings of the 26th Joint Propulsion Conference (1990) 2135.

- [8] S. Mohler, Wind-US flow calculations for the M2129 S-duct using structured and unstructured grids. In 42nd AIAA Aerospace Sciences Meeting and Exhibit, (2004) 525.
- [9] C.F. Smith, S.D. Podleskif, W.S. Barankiewicz, S.Z. Zeleznik, Comparison of F/A-18A inlet flow analyses with flight data, *Journal of Aircraft* 33 (1996) 457–462.
- [10] P.E.H. Abrahamsent, B.A.P. Reifi, L. Szetrar, J.B. Fossdalt, Air Intake Studies: Experimental measurements and computational modelling. In: *Proceedings of RTO AVT Symposium on Missile Aerodynamics*, (1998).
- [11] E.L. Goldsmith, J. Seddon, Practical intake aerodynamic design. Amer Inst of Aeronautics & Astronautics, Washington D.C. (1993).
- [12] B. Gunston, (ed.) *Jane's aero-engines*. Jane's Information Group (2001).
- [13] A.M. Nili, F. Ghadak, M. Mohammadi, A. Nejati, 2-D aerodynamic design of turbojet engine S-shaped air intake considering the engine nose effects (2011) 59–69.
- [14] F. U. Manual, *Fluent user's guide*, Fluent Inc, Lebanon 68 (2005).
- [15] <https://www.grc.nasa.gov>.
- [16] S.N. Shojaee, H.A. Hazaveh, Investigation of total pressure distribution at aerodynamic interface plane of an "S-shaped" air intake at sideslip condition, *International Journal of Natural and Engineering Sciences* 6 (2012) 1307–1149.